# Unidirectional Adsorbate Motion on a High-Symmetry Surface: "Walking" Molecules Can Stay the Course

Ki-Young Kwon,[1] Kin L. Wong,[1] Greg Pawin,[1] Ludwig Bartels,[1,*] Sergey Stolbov,[2] and Talat S. Rahman[2]

[1]*Pierce Hall, University of California, Riverside, California 92521, USA*
[2]*Department of Physics, Kansas State University, Manhattan, Kansas 66506, USA*

Step edges and low-symmetry faces of metal crystals can restrict the diffusive motion of adsorbates, yet they offer little flexibility with regards to the location and/or direction of the guided motion. We show inherently unidirectional motion of an organic molecule on a high-symmetry thermodynamic-equilibrium metal surface [Cu(111)]. Sequential placement of the substrate linkers of 9,10-dithioanthracene prevents it from rotating or veering off course. A combination of low temperature scanning tunneling microscopy and density functional theory simulations provide atomistic insight.

PACS numbers: 68.43.Bc, 68.35.Fx, 68.43.Jk, 82.37.Gk

Since the scanning tunneling microscope (STM) was used to spell letters from individual xenon atoms [1], there has been the dream that ultimately this technique will lead to the assembly of molecular-scale machinery on surfaces. In 1996, Gimzewski's group proposed that computational tasks may be accomplished by arrangement of molecules in an abacus fashion [2]. Although atomic-precision placement of atoms or molecules on a flat high-symmetry surface is possible [3], for rapid high-precision manipulation they employed the intrinsic guidance provided by a substrate step edge. Alternatively, unidirectional adsorbate motion is found on highly anisotropic surfaces [e.g., fcc(110)] of metal crystals [4–7]. However, if unidirectional motion were possible at *arbitrary* locations on high-symmetry thermodynamic-equilibrium surfaces, then the size of a regular molecular array for computational purposes is only limited by the extent of the substrate terraces on the scale of thousands of nm [2]. Moreover, signaling between a surface structure and a neighboring one at a specific relative location may be achieved by means of release of molecules that diffuse in a strictly linear fashion between them. Here we report on the dynamics of 9,10-dithioanthracene on Cu(111), which realizes unidirectional motion along any of the three substrate high-symmetry axes. 9,10-dithioanthracene (DTA) is designed to have two thiol linkers to the substrate, which, due to the molecular geometry, move in alternation so that the stationary one guides the motion of the mobile one in the direction of the next step and prevents the molecule from rotating or veering off course.

We synthesized acetyl-protected 9-thioanthracene (TA) and DTA following Ref. [8], which will be described in detail elsewhere. Sample preparation proceeds by thermal evaporation of DTA or TA onto a clean Cu(111) surface precooled to 90 K at a base pressure of $<10^{-10}$ torr. Clean removal of the acetyl protection is accomplished by post-deposition annealing to room temperature (RT) with real-time mass-spectrometric monitoring. Images shown in this

study were obtained after renewed cooling to 90 K and below, as indicated. DTA/Cu(111) forms rows of molecules [Fig. 1(b)], in which each molecule appears as an elongated shape [Fig. 1(c)] with slightly elevated ends. Two low protrusions, one on each side, resemble the thiol groups of thiophenol/Cu(111) [9]. This suggests that DTA lies flat on the surface with both sulfur atoms attached to the substrate. For comparison, we show an image of a TA molecule [Fig. 1(d)], which resembles DTA except that the second thiol group is missing. Both for TA and DTA we find that the anthracene moiety is always aligned with a substrate high-symmetry (i.e., [$\bar{1}$10]-like) directions. Because of the threefold symmetry of the substrate, DTA and TA can adsorb in three different rotational orientations.

After cooling to 50–70 K, the diffusion of individual DTA molecules can be followed by STM. In particular, we
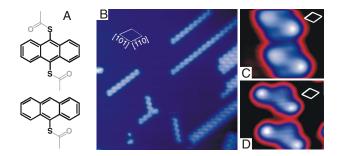


FIG. 1 (color online). (a) 9,10-dithioacetylanthracene and 9-thioacetylanthracene. The acetyl protection group (gray) is required to prevent poly-/dimerization during thermal deposition and it is removed by RT annealing after deposition onto Cu(111). (b) Cu(111) surface with rows of DTA molecules after deposition at 90 K and annealing (23 nm by 23 nm, $I = 110$ pA, $Vs = -1.7$ V, 80 K). (c),(d) High-resolution STM images of DTA and TA. The anthracene moiety (with the terminal benzene rings appearing bright) is aligned with the substrate high-symmetry axis and the thiol substrate linkers appear as small protrusions on the side ($20 \times 17$ Å, $I = 220/97$ pA, $Vs = -1.0/-1.5$ V, 80/83 K).

observe that every DTA molecule diffuses exclusively along the substrate high-symmetry direction indicated by its anthracene moiety. Figs. 2(a) and 2(c) show two successive images of isolated DTA molecules as well as of a stationary row of molecules on the right, which serve as a registry marker. The difference image [Fig. 2(b)] reveals that between acquisition of the images each molecule stepped along the $[\bar{1}10]$-like direction aligned with its anthracene moiety by 2.55 Å, i.e., the spacing between adjacent Cu atoms. In >5000 recorded diffusion events (a sample of which is shown in Ref. [10]) we did not witness a single instance in which the molecule executed any surface motion other than moving in the direction indicated by its anthracene moiety. TA molecules, which have only one sulfur substrate linker, do not show unidirectional diffusion, but rather a preference for rotation around their sulfur atom. Temperature dependent measurements of DTA diffusion reveal a barrier of 130 meV and an attempt frequency of 4.0 GHz [Fig. 2(d)].

We also attempted lateral manipulation of a DTA molecule using the STM tip as a nanoscale actuator. Even at 10 K, manipulation is quite facile ($U_b = -250$ mV, $I = 0.5$ nA $\rightarrow R = 500$ MΩ) along the substrate high-symmetry axis aligned with the molecule. However, rotation of the molecule or translation at an angle to its axis could not be achieved even at 1/10 of the mentioned gap resistance.

In pursuit of the origin of the restricted diffusion, we performed density functional theory (DFT) calculations of the molecule's adposition on the surface using a variety of substrate unit cells ranging from a $5 \times 3$ cell with 2 substrate layers (532) to a $6 \times 4$ cell with 4 substrate layers (644). Each time we started out from several different initial molecular orientations and adpositions and found consistently two different minima of the adsorption potential. These calculations use the generalized-gradient ap-

proximation [11] for the exchange-correlation functional and the plane-wave pseudopotential method [12] with ultrasoft pseudopotentials [13]. The structures were relaxed until the forces acting on each atom were less than 0.02 eV/Å and 0.05 eV/Å for Figs. 3 and 4, respectively.

Figure 3(a) shows the minimum energy position of DTA, which places the aryl moiety parallel to the substrate high-symmetry direction and is, thus, compatible with the STM data. As a result of a mismatch between the intramolecular S-S distance and the substrate periodicity, the sulfur atoms are found to occupy different adsorption sites: the sulfur atom labeled 1 in Fig. 3(a) (S1) is located between the bridge and the hcp hollow site (which resembles the adsorption geometry of thiophenol/Cu(111) [14]), whereas sulfur 2 (S2) resides close to an on-top site. In this configuration, the carbon atoms of the anthracene ring system are well aligned with the substrate in a fashion similar to the anthracene adsorption geometry on Cu(111) under solution [15]. Calculations for TA (which has no S2) result in a similar adposition of its sulfur atom and anthracene moiety.

A slight rotation of DTA around S1 in either direction brings both sulfur atoms close to energetically favorable [14] near-bridge sites, yet it renders the anthracene adsite less symmetric, which makes the interaction between the anthracene $\pi$ system [16] and the substrate energetically less favorable. This position corresponds to the second energetic minimum of our DFT calculations [Fig. 3(b)]. It is separated from the first one by a small barrier of $\approx$ 30 meV. The absence of STM images showing DTA molecules misaligned to the substrate high-symmetry direction from our diffusion measurements rule out that Fig. 3(b) represents the equilibrium adsorption position, yet the calculations predict it to be slightly lower in energy than the first one. We tentatively attribute the preference of the calculations for an optimal S2 adsite over an optimal
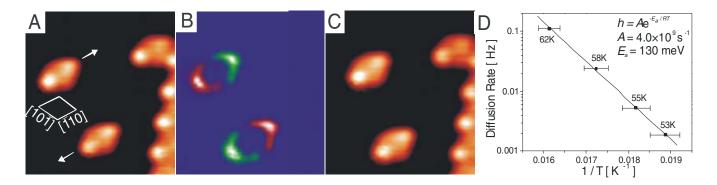


FIG. 2 (color online).　(a), (c) show STM images ($48 \times 48$ Å, $I = 80$ pA, $Vs = -3.0$ V, 55 K, 55 s/image) of two isolated DTA molecules and a DTA island (right). The difference image (b) shows that both molecules diffused along the $[\bar{1}10]$ axis in opposite direction each by one Cu-Cu atom spacing of 2.55 Å. We followed >5000 such diffusion events and observed exclusively diffusion in the direction of the anthracene moiety. Panel (d) shows an Arrhenius plot obtained by measurement of DTA diffusion between 53 and 62 K. The vertical error bars are omitted, because they are each smaller than the square symbols used to indicate the data point. The horizontal error bars reflect a potential error of the temperature calibration by $+/-1$ K. Care was taken to avoid any tip influence on the observed diffusion rate.
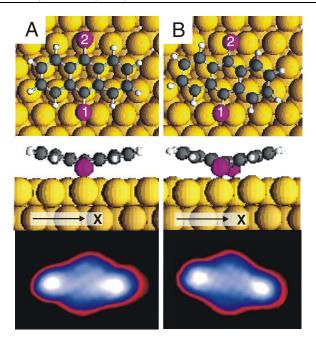
FIG. 3 (color online). DFT calculations yield an adsorption minimum of DTA, in which the two sulfur atoms (labeled 1 and 2) occupy different adsites while the aromatic ring is aligned with the substrate atomic high-symmetry direction as observed in Figs. 1 and 2. The outer rings of the aromatic moiety are bent upwards, which agrees with the appearance of DTA in STM images. A rotation around S1 leads to a second adsorption minimum (b). Here both sulfur atoms occupy favorable near-hollow sites whereas the anthracene moiety comes to rest in an unfavorable low-symmetry orientation. This orientation is not observed at temperatures allowing for thermal movement of DTA. The bottom images show a DTA molecule before and after it was transferred by the STM tip from position (a) to (b) in experiments conducted at 10 K.

time one or both of the sulfur atoms moves $<0.2$ Å in the $X$ direction of Fig. 3, i.e., along the [1$\underline{1}$0]-like direction indicated by the anthracene moiety of Fig. 3(a). At each adposition we minimize the total energy of the DTA/substrate system while restraining only the $x$ positions of S1, S2, and of one copper atom of the bottom layer of a 533 or 644 cell. Figure 4 shows on the $x$ and $y$ axes the $x$ positions of S1 and S2, respectively, and on the $z$ axis the resultant potential energy. If DTA diffused from one adsite to the next (at 2.55 Å separation) by moving the sulfur atoms in unison, then we would find a potential energy trough running diagonally across the $x$-$y$ plane. By contrast, we find a trough that runs alternately parallel to the axis indicating movement of S1 and to the axis indicating movement of S2. In other words, during diffusion from one adsite to the next, DTA first rotates around S1 so that S2 moves onto the second minimum of the adsorption potential. At that point, the direction of the potential energy trough turns and further rotation around S1 becomes energetically prohibitive. Consequently, the molecule either rotates back around S1 to return to its initial position, or S2 becomes the quasistationary substrate linker and DTA rotates around it so that S1 moves forward. On this move DTA passes through the diffusion transition state, which exceeds the minimum energy position of the diffusion potential by $\approx 160$ meV, in reasonable agreement with the experimental value of 130 meV. Finally, the molecule rotates again around S1 to be aligned with substrate high-symmetry direction.

In our calculation we alternately move the molecule, minimize the energy, and use the resultant configuration as a starting point for the next cycle. We restrict the sampled configuration space to those molecular setups that can be reached without traversing a barrier in excess of 300 meV.
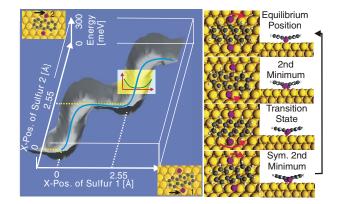
anthracene adsite to the omission of electron-electron correlations in our calculations, which can be relevant for the description of a $\pi$-bonded system at highest fidelity. Working at 10 K (i.e., far below the regime of thermal diffusion), molecules can be transferred into this orientation by means of the STM tip (bottom of Fig. 3).

The adjacency of an additional energetic minimum on each side of the experimentally-confirmed adsorption geometry suggests that the DTA adsite is governed by a delicate balance between antagonistic forces that try to optimize the adpositions of either S2 or the anthracene moiety. The impact of this balance on the diffusion barrier of DTA is underlined by the experimental observation that DTA diffusion occurs at temperatures as low as 50 K, whereas 80 K is required for rotation/diffusion of TA, which does not have to accommodate S2.

In order to elucidate how unidirectional diffusion results from this careful balance, we calculated the potential energy surface governing diffusion of DTA on Cu(111) by iteratively rotating/translating the molecule, so that each



FIG. 4 (color online). The potential energy trough during diffusion of S1 and S2 along the $X$ direction of Fig. 3. The minimum energy trajectory (blue line) initially follows one coordinate (i.e., S2 moves and S1 is stationary) and then the other coordinate (i.e., S1 moves and S2 is stationary). This trough is generated by $>250$ minimizations of DTA and a 533 substrate cell. On the right, four molecular orientations along the minimum energy trajectory are shown.

We wish to point out that the *y* and *z* positions of the sulfur atoms were not fixed during energy minimization. Thus, the molecule was not restricted from rotating permanently around one sulfur atom or from diffusing transversal to the substrate high-symmetry line, if this were energetically favorable.

The sequential motion of DTA's thiol linkers (Fig. 4) bears striking resemblance to bipedal locomotion (e.g., human walking), with one foot always on the ground to guide the motion of the other [10]. In the case of DTA, this guidance prevents the molecule from rotating beyond the second adsorption minimum and ensures that—once this minimum is reached—the stationary substrate linker becomes the mobile one, if the motion is to continue. As a consequence, DTA moves constantly along one line similar to a shuttle on a loom.

As an outlook, we note that recent research indicates that the adaptation of biological or biomimetic systems for transport of individual molecules holds important prospects [17,18]. In contrast to Ref. [2], such systems provide transport on the molecular scale while avoiding applicability and throughput limitations imposed by the (sequential) nature of STM (manipulation); they also offer facile integration into other biomimetic nanomechanical schemes. However, those systems require microtubules or lithographic surface patterns for guidance. Our results suggest a far more facile concept for realizing guidance and require no more than thermodynamic equilibrium surfaces of Cu, which can be created by deposition of copper on "any" flat surface. In combination with a controllable source of motion, e.g., the photochemical realization described in Ref. [19], encoding of guided diffusion in the geometric relation between admolecule and substrate may ultimately facilitate the setup of complex functional machinery on the nanoscale.

*Corresponding author.
Electronic address: Ludwig.Bartels@UCR.EDU

[1] D. M. Eigler and E. K. Schweizer, Nature (London) **344**, 524 (1990).
[2] M. Cuberes, R. Schlittler, and J. Gimzewski, Appl. Phys. Lett. **69**, 3016 (1996).
[3] J. Stroscio and R. Celotta, Science **306**, 242 (2004).
[4] R. Otero *et al.*, Nat. Mater. **3**, 779 (2004).
[5] M. Schunack *et al.*, J. Chem. Phys. **117**, 6259 (2002).
[6] S. Stranick, M. Kamna, and P. Weiss, Science **266**, 99 (1994).
[7] L. Gross *et al.*, Chem. Phys. Lett. **371**, 750 (2003).
[8] J. Tour *et al.*, J. Am. Chem. Soc. **117**, 9529 (1995).
[9] K. Wong *et al.*, J. Am. Chem. Soc. **126**, 7762 (2004).
[10] See EPAPS Document No. E-PRLTAO-073542 for a STM movie of DTA diffusion at 55 and 67 K as well as animation of the diffusion process. This document can be reached via a direct link in the online article's HTML reference section or via the EPAPS homepage (http://www.aip.org/pubservs/epaps.html).
[11] J. Perdew and Y. Wang, Phys. Rev. B **45**, 13 244 (1992).
[12] M. Payne *et al.*, Rev. Mod. Phys. **64**, 1045 (1992).
[13] D. Vanderbilt, Phys. Rev. B **41**, 7892 (1990).
[14] K. Wong *et al.*, Langmuir **20**, 10 928 (2004).
[15] L. Wan and K. Itaya, Langmuir **13**, 7173 (1997).
[16] W. Zhao, W. Wei, and J. White, Surf. Sci. **547**, 374 (2003).
[17] H. Hess *et al.*, Nano Lett. **1**, 235 (2001).
[18] H. Hess *et al.*, Nano Lett. **3**, 1651 (2003).
[19] Z. Wang, Phys. Rev. E **70**, 031903 (2004).